Constant Power Control Of 15 DFIG Wind Turbines With Superconducting Magnetic Energy Storage System

V.Krishnamurthy [1], Ch.Rajesh Kumar [2]

[1]*Department of electrical and electronics engineering, Narayana Engineering College, Nellore,Ap,India.*

2 Associate proffesor Department of electrical and electronics engineering, Narayana Engineering College, Nellore,Ap,India.

***Abstract*- With the increasing penetration of wind power into electric power grids, energy storage devices will be required to dynamically match the intermittency of wind energy. This paper proposes a novel two-layer constant power control scheme for a wind farm equipped with doubly fed induction generator (DFIG) wind turbines. Each DFIG wind turbine is equipped with a superconducting magnetic energy storage system (ESS) and is controlled by the low-layer wind turbine generator (WTG) controllers and coordinated by a high-layer wind farm supervisory controller (WFSC). The WFSC generates the active power references for the low-layer WTG controllers according to the active power demand from or generation commitment to the grid operator; the low-layer WTG controllers then regulate each DFIG wind turbine to generate the desired amount of active power, where the deviations between the available wind energy input and desired active power output are compensated by the ESS. Simulation studies are carried out in MATLAB/SIMULINK on a wind farm equipped with 15 DFIG wind turbines to verify the effectiveness of the proposed control scheme.**

***Keywords*- Constant power control (CPC), doubly fed induction generator (DFIG), superconducting magnetic energy storage, supervisory controller, wind turbine**

I.INTRODUCTION

In the early 1980's, the Department of Non-conventional Energy Sources (DNES) came into existence with the aim to reduce the dependence of primary energy sources like coal, oil etc in view of the Country's energy security. The DNES became Ministry of Non-conventional Energy Sources (MNES) in the year 1992 and now from 2006, the Ministry was renamed as Ministry of New & Renewable Energy (MNRE).The growth of Renewable Energy in India is enormous and Wind Energy proves to be the most effective solution to the problem of depleting fossil fuels, importing of coal, greenhouse gas emission, environmental pollution etc. Wind energy as a renewable, non-polluting and affordable source directly avoids dependency of fuel and transport, can lead to green and clean electricity.

With an installed capacity of 19 GW (Mar 2013) of wind energy, Renewable Energy Sources (excluding large Hydro) currently accounts for 12.5% i.e. 27.5 GW of India's overall installed power capacity. Wind Energy holds the major portion of 70% among renewable and continued as the largest supplier of clean energy.

In its 12th Five Year Plan (2012-2017), the Indian Government has set a target of adding 18.5 GW of renewable energy sources to the generation mix out of which 11 GW is the Wind estimation and rest from renewable sources like Solar 4 GW and others 3.5 GW. The industry has represented its capability with good policy frame work to achieve a reference target of 15,000 MW, realistic target of 20,000 MW and an aspirational target of 25,000 MW in the plan period of 2012-2017.At such high levels of penetration, it will become necessary to require WTGs to supply a desired amount of active power to participate in automatic generation control or frequency regulation of the grid [3]. However, the intermittency of wind resources can cause high rates of change (ramps) in power generation [4], which is a critical issue for balancing power systems. Moreover, to optimize the economic performance of power systems with high penetrations of wind power, it would be desired to require WTGs to participate in unit commitment, economic dispatch, or electricity market operation [5]. In practice, short-term wind power prediction [6] is carried out to help WTGs provide these functions. To enable WTGs to effectively participate in frequency and active power regulation, unit commitment, economic dispatch, and electricity

market operation, energy storage devices will be required to dynamically match the intermittency of wind energy. In [8], the authors investigated and compared different feasible electric energy storage technologies for intermittent renewable energy generation, such as wind power. Currently, pumped water and compressed air are the most commonly used energy storage technologies for power grids due to their low capital costs [9]. However, these two technologies are heavily dependent on geographical location with relatively low round-trip efficiency. Compared with their peers, batteries, supercapacitors and superconducting magnetic energy storage are more efficient, have a quicker response to demand variations, and are easy to develop and ubiquitously deployable. Compared superconducting magnetic energy storage batteries and supercapacitors has a very low energy storage density leading to very high capital costs for large scale applications. So a superconducting magnetic energy storage system is a good candidate for short-term energy storage that enables WTGs to provide the function of frequency regulation and effectively participate in unit commitment and electricity market operation. This paper proposes a novel two-layer constant power control (CPC) scheme for a wind farm equipped with doubly fed induction generator (DFIG) wind turbines, where each WTG is equipped with a superconducting magnetic energy storage system(ESS). The CPC consists of a high-layer wind farm supervisory controller (WFSC) and low-layer WTG controllers. The high layer WFSC generates the active power references for the low layer WTG controllers of each DFIG wind turbine according to the active power demand from the grid operator.

The low-layer WTG controllers then regulate each DFIG wind turbine to generate the desired amount of active power, where the deviations between the available wind energy input and desired active power output are compensated by the ESS. Simulation studies are carried out in MATLAB/SIMULINK for a wind farm equipped with 15 DFIG wind turbines to verify the effectiveness of the proposed control scheme.

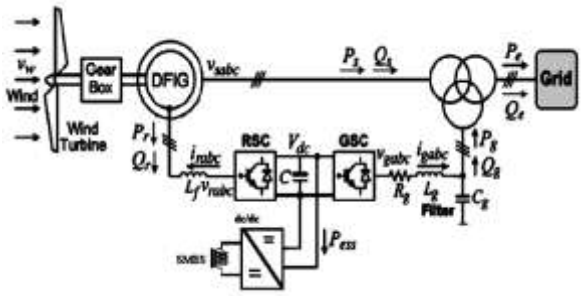

Fig.1. Configuration of a DFIG wind turbine equipped with a superconducting magnetic ESS connected to a power grid.

II. DFIG WIND TURBINE WITH ENERGY STORAGE

Fig. 1 shows the basic configuration of a DFIG wind turbine equipped with a superconducting magnetic ESS. The low-speed wind turbine drives a high-speed DFIG through a gearbox. The DFIG is a wound-rotor induction machine. It is connected to the power grid at both stator and rotor terminals. The stator is directly connected to the grid, while the rotor is fed through a variable-frequency converter, which consists of a rotor-side converter (RSC) and a grid-side converter (GSC) connected back to back through a dc link and usually has a rating of a fraction (25%–30%) of the DFIG nominal power. As a consequence, the WTG can operate with the rotational speed in a range of ±25%–30% around the synchronous speed, and its active and reactive powers can be controlled independently.

In this paper, an ESS consisting of a SMES systems basically consist of a large coil, AC/DC converters and cooling units. The conductors used in the coil are superconductors, and therefore powerful cooling units need to be employed to maintain the superconductivity feature of the conductors. AC/DC converters convert the available AC voltage into DC form which is required for energy storage. By proper control, the AC/DC converters invert the stored DC energy into AC form so that it can be utilized. The ESS serves as either a source or a sink of active power and therefore contributes to control the generated active power of the WTG.

The use of an ESS in each WTG rather than a large single central ESS for the entire wind farm is based on two reasons. First, this arrangement has a high reliability because the failure of a single ESS unit does not affect the ESS units in other WTGs. Second, the use of an ESS in each WTG can reinforce the dc bus of the DFIG converters during transients, thereby enhancing the low-voltage ride through capability of the WTG [10].

III. CONTROL OF INDIVIDUAL DFIG WIND TURBINE

The control system of each individual DFIG wind turbine generally consists of two parts: 1) the electrical control of the DFIG and 2) the mechanical control of the wind turbine blade pitch angle and yaw system. Control of the DFIG is achieved by controlling the

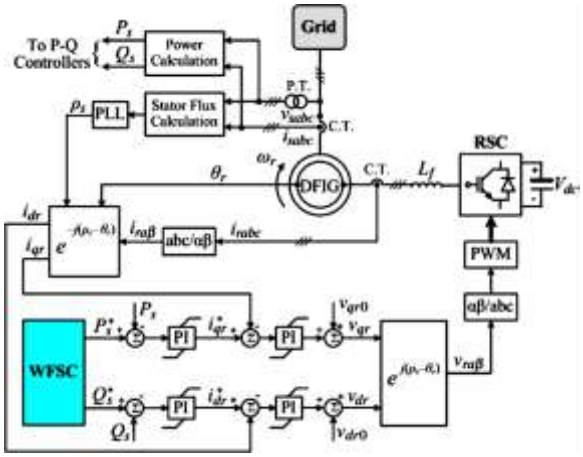

Fig. 2. Overall vector control scheme of the RSC.

RSC, the GSC, and the ESS (see Fig. 1). The control objective of the RSC is to regulate the stator-side active power *Ps* and reactive power *Qs* independently. The control objective of the GSC is to maintain the dc-link voltage *V*dc constant and to regulate the reactive power *Qg* that the GSC exchanges with the grid.

A. Control of the RSC

Fig. 2 shows the overall vector control scheme of the RSC, in which the independent control of the stator active power *Ps* and reactive power *Qs* is achieved by means of rotor current regulation. Therefore, the overall RSC control scheme consists of two cascaded control loops. The outer control loop regulates the stator active and reactive powers independently, which generates the reference signals $i_{dr}^{*}$and i_{qr}^{*} of the *d*- and *q*-axis current components, respectively, for the inner-loop current regulation. The outputs of the two current controllers are compensated by the corresponding cross-coupling terms v_{dr0} and v_{qr0} , respectively, to form the total voltage signals v_{dr} and v_{qr}. They are then used by the pulse width modulation (PWM) module to generate the gate control signals to drive the RSC. The reference signals of the outer-loop power controllers are generated by the high-layer WFSC.

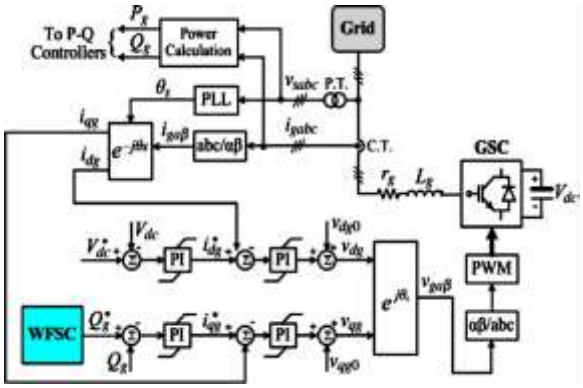

Fig.3. Overall vector control scheme of the GSC.

Fig. 3 shows the overall vector control scheme of the GSC,in which the control of the dc-link voltage *V*dc and the reactive power *Qg* exchanged between the GSC and the grid is achieved by means of current regulation. Again, the overall GSC control scheme consists of two cascaded control loops.

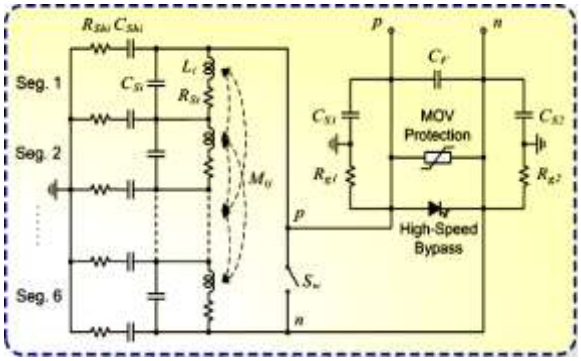

. Fig.4 equivalent circuit of the SMES coil

The outer control loop regulates the dc-link voltage *V*dc and the reactive power *Qg*, respectively, which generates the reference signals $i*dg$ and $i* qg$ of the *d*- and *q*-axis current components, respectively, for the inner-loop current regulation. The outputs of the two current controllers are compensated by the corresponding crosscoupling terms *vdg*0 and *vqg*0, respectively, to form the total voltage signals *vdg* and *vqg*. They are then used by the PWM module to generate the gate control signals to drive the GSC. The reference signal of the outer-loop reactive power controller is generated by the high-layer WFSC.

C. Configuration and Control of the ESS

Fig. 4 shows the configuration and control of the ESS. The ESS consists of a superconducting magnetic coil and a two-quadrant dc/dc converter connected to the dc link of the DFIG. The equivalent circuit of the SMES coil makes use of a lumped parameters network represented by a six-segment model comprising self inductances (*Li*), mutual couplings between segments *i* and *j*(*Mij*), ac loss resistances (*Rshi*), skin effect-related resistances (*Rsi*), turn-ground (shunt—*Cshi*) and turn-turn capacitances (series— *Csi*) , over a frequency range from dc to several thousand Hertz. The inclusion of surge capacitors (*CS1* and *CS2*) and a filter capacitor *CF* in parallel with grounding balance resistors (*Rg1* and *R*g2) allows reducing the effect of resonances. A metal oxide semiconductor protection for transient voltage surge suppression is included between the SMES model and the dc/dc converter. Coupling is the desirable or undesirable transfer of energy from one medium, such as a metallic wire or an optical fiber, to another medium, including fortuitous transfer(14).For mutual inductance, measure the inductance of the primary and secondary in series, and then interchange the connections of one winding for a second reading. Apply the equation below:

$$M = \frac{1}{4}\left(L_{series+} - L_{series-}\right)$$

For coupling, measure the primary and secondary separately then apply the equation below:

$$k = \frac{M}{\sqrt{L_p L_s}}$$

In general, that which is not mutual inductance must be leakage inductance, but resistive losses and capacitive effects will prevent perfect agreement between the formulas. Refer to a text containing the general coupling solution for more exact results.

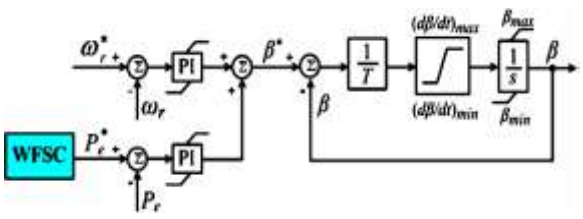

Fig.5. Blade pitch control for the wind turbine.

D. Wind Turbine Blade Pitch Control

Fig. 5 shows the blade pitch control for the wind turbine, where ω_r and P_e (= P_s + P_g) are the rotating speed and output active power of the DFIG, respectively. When the wind speed is below the rated value and the WTG is required to generate the maximum power, ω_r and P_e are set at their reference values, and the blade pitch control is deactivated. When the wind speed is below the rated value, but the WTG is required to generate a constant power less than the maximum power, the active power controller may be activated, where the reference signal P_e^* is generated by the high-layer WFSC and P_e takes the actual measured value. The active power controller adjusts the blade pitch angle to reduce the mechanical power that the turbine extracts from wind. This reduces the imbalance between the turbine mechanical power and the DFIG output active power, thereby reducing the mechanical stress in the WTG and stabilizing the WTG system. Finally, when the wind speed increases above the rated value, both ω_r and P_e take the actual measured values, and both the speed and active power controllers are activated to adjust the blade pitch angle.

IV. WIND FARM SUPERVISORY CONTROL

The objective of the WFSC is to generate the reference signals for the outer-loop power controllers of the RSC and GSC, the controller of the dc/dc converter, and the blade pitch controller of each WTG, according to the power demand from or the generation commitment to the grid operator.

The optimal rotational speed $\omega_{ti,\text{opt}}$ in radians per second of the wind turbine can be determined, which is proportional to the wind speed v_{wi} at a certain pitch angle β_i

$$\mathrm{w_{ti,ot}} = \mathrm{k}(\beta_\mathrm{i})\mathrm{v_{wi}} \qquad (3)$$

where *k* is a constant at a certain value of β_i.Then, the maximum mechanical power *Pmi*,max that the wind turbine extracts from the wind can be calculated by the well-known wind turbine aerodynamic characteristics

$$P_{mi,max} = \frac{1}{2}\rho_i A_r v_{wi}^3 C_{pi}\left(\lambda_{i,opt},\beta_i\right) \quad (4)$$

where ρ_i is the air density in kilograms per cubic meter; A_r =πR^2 is the area in square meters swept by the rotor blades, with *R* being the blade length in meters; and C_{Pi} is the power. In (4), $\lambda_{i,\text{opt}}$ is the optimal tip-speed ratio when the wind turbine rotates with the optimal speed ω_{ti},opt at the wind speed v_{wi}. Given $P_{mi,\text{max}}$, the maximum active power $P_{ei,\text{max}}$

generated by the WTG can be estimated by taking into account the power losses of the WTG

$P_{ei,\max} = P_{mi,\max} - P_{Li} = P_{si,\max} + P_{ri,\max}$ (6)

where P_{Li} is the total power losses of WTG i, which can be estimated by the method in $P_{si,\max}$ and $P_{ri,\max}$ are the maximum DFIG stator and rotor active powers of WTG i, respectively. In terms of the instantaneous variables in Fig.1, the stator active power P_s can be written in a synchronously rotating dq reference frame as follows:

$$P_s = \frac{3}{2}\left(V_{ds} i_{ds} + V_{qs} i_{qs}\right) \quad (7)$$

where v_{ds} and v_{qs} are the d- and q-axis voltage components of the stator windings, respectively; ids and i_{qs} are the stator d- and q-axis current components, respectively; i_{dr} and i_{qr} are the rotor d- and q-axis current components, respectively; ω_s is the rotational speed of the synchronous reference frame; and r_s and L_m are the stator resistance and mutual inductance, respectively. Similarly, the rotor active power is calculated by

$$P_r = \frac{3}{2}\left(V_{dr} i_{dr} + V_{qr} i_{qr}\right) \quad (8)$$

where v_{dr} and v_{qr} are the d- and q-axis voltage components of the rotor windings, respectively; s is the slip of the DFIG defined by

$s = (\omega_s - \omega_r)/\omega_s$ (9)

where ω_r is the DFIG rotor speed. (7) and (8) yield

$$P_r = -sP_s \quad (10)$$

According to (6) and (10) $P_{si,\max}$ and $P_{ri,\max}$ of each WTG can be determined. Then, the total maximum mechanical power $P_{m,\max}$, DFIG output active power $P_{e,\max}$, and stator

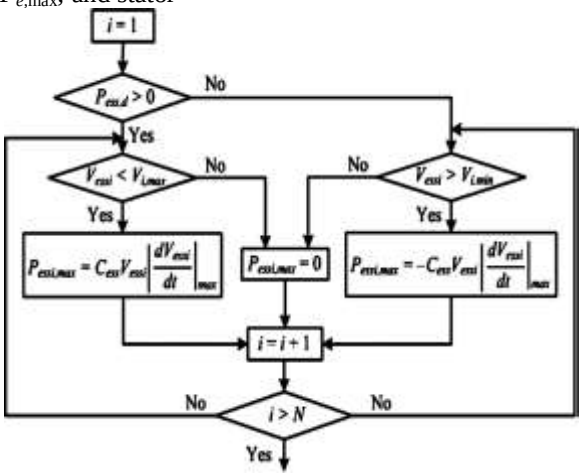

Fig.6. Flowchart of determination of $P_{essi,\max}$ for each WTG.

active power $P_{s,\max}$ of all WTGs in the wind farm can be calculated as

$$P_{m,max} = \sum_{i=1}^{N} P_{mi,max} \quad (12)$$

$$P_{e,max} = \sum_{i=1}^{N} P_{ei,max} \quad (13)$$

$$P_{s,max} = \sum_{i=1}^{N} P_{si,max} \quad (14)$$

In order to supply constant power P_d to the grid, the deviation $P_{ess,d}$ between the demand/commitment P_d and the maximum generation $P_{e,\max}$ is the power that should be stored in or supplied from the ESSs of the WTGs

$$P_{ess,d} = P_{e,max} - P_d \quad (15)$$

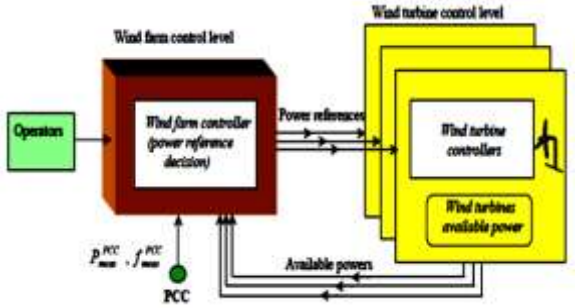

Fig.8. Proposed two-layer CPC scheme for the wind farm.

V. SIMULATION RESULTS

Simulation studies are carried out for a wind farm with 15 DFIG wind turbines to verify the effectiveness of the proposed control scheme under various operating conditions. Each DFIG wind turbine (see Fig. 1) has a 3.6-MW power capacity. The total power capacity of the wind farm is 54 MW.

A. CPC During Variable Wind Speed Conditions

Fig. 9 shows without energy storage system. Fig.10 shows the wind speed profiles of WTG1 (*vw*1), WTG2 (*vw*2), and WTG3 (*vw*3).Fig. 11.shows the variations of the wind power output when the DFIG is not equipped with energy storage system.Fig.12 shows the DFIG equipped with energy storage system and the Fig.13 shows the comparision of wind farm output and the demand from the grid operator

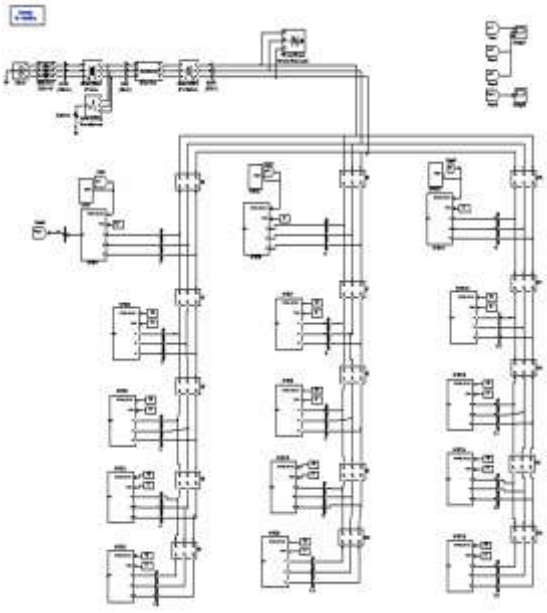

Fig. 9. Without energy storage system

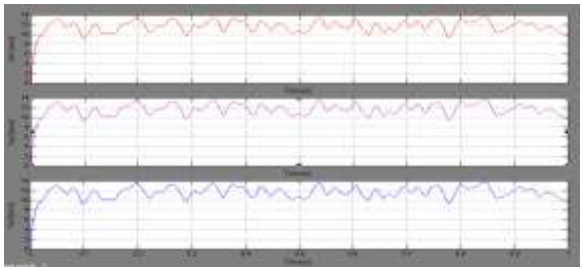

Fig.10: Wind speed profiles of WTG1, WTG2,WTG3

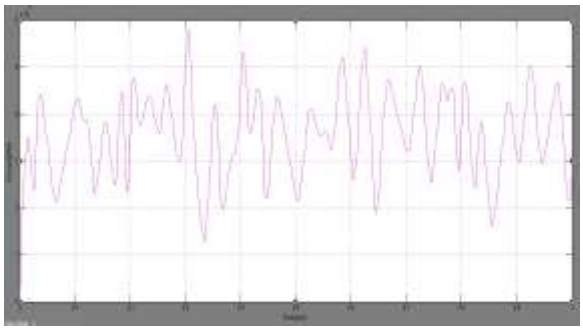

Fig. 11 Wind farm power output without ESSs and the proposed CPC scheme.

B .DFIG Wind Turbine With SMES System

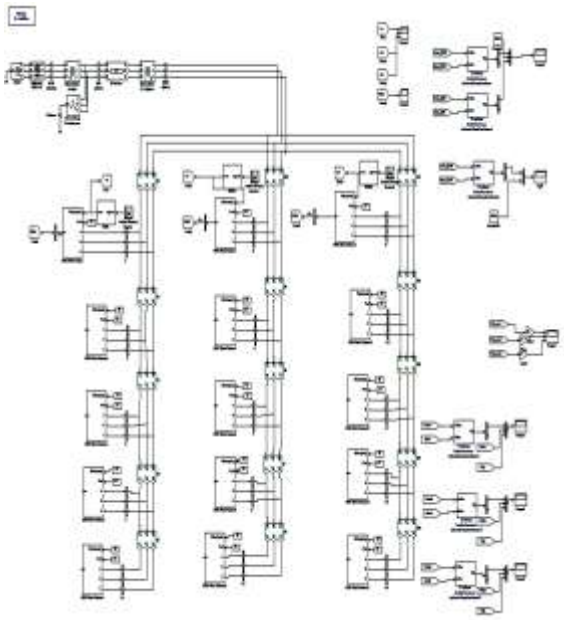

Fig.12.With energy storage system

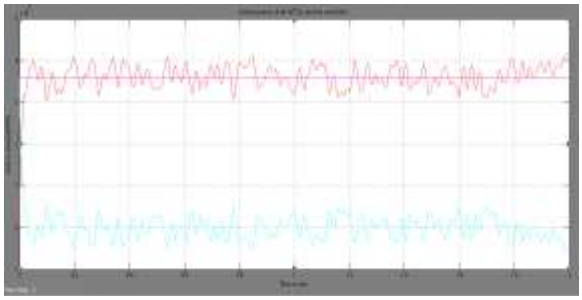

Fig.15. : Active powers of all WTGs and the wind farm

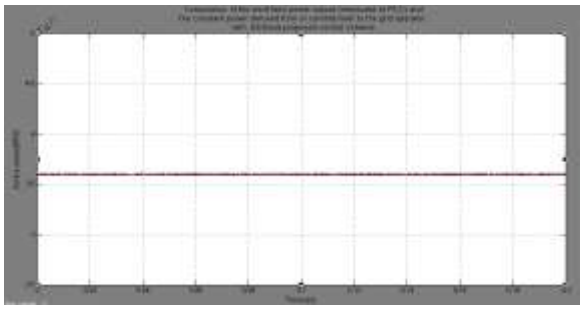

Fig.16. Comparison of the wind farm power output (measured at PCC) and the constant power demand from or commitment to the grid operator: With ESSs and the proposed CPC scheme.

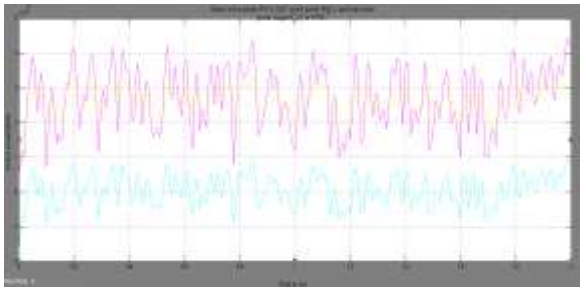

Fig.17. Stator active power (*Ps*1), GSC active power (*Pg*1), and total active power output (*Pe*1) of WTG1.

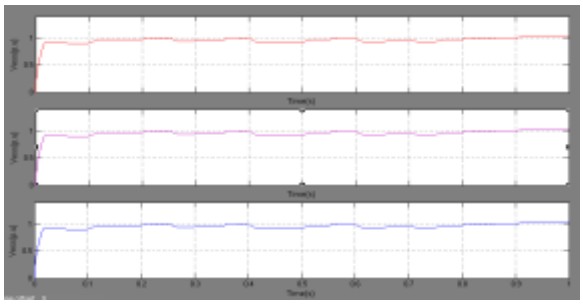

Fig.20. Voltages of the superconducting magnetic energy storage system of WTG1,WTG2, andWTG3

C. Power Tracking Performance When The Demand Is Step Changed

Under the same wind conditions as in the previous tests, the power demand from or commitment to the grid operator is now step changed from time to time. The wind farm is controlled by the proposed CPC scheme to track the variations of the power demand

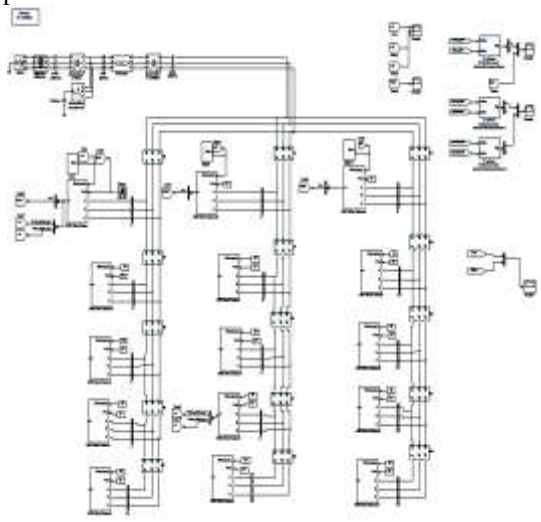

Fig.21Power tracking during step change in demand

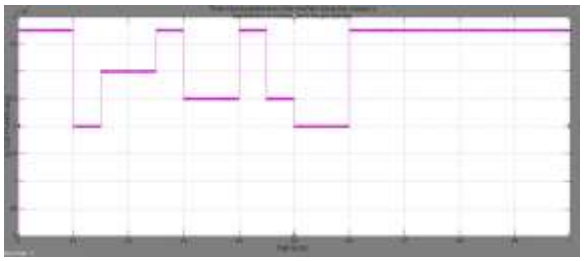

Fig.26. Power tracking performance of the wind farm during step changes in demand from or commitment to the grid operator.

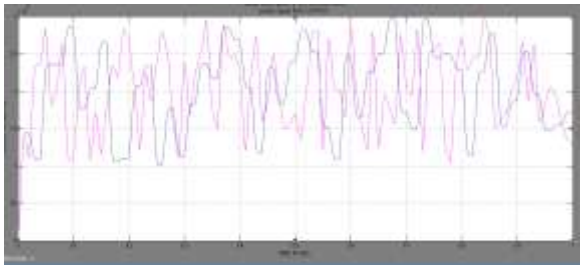

Fig.22. Total active power outputs ofWTG1 (*Pe*1) andWTG5 (*Pe*5) during step changes in demand from or commitment to the grid operator.

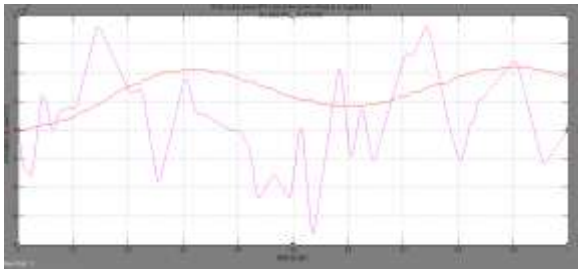

Fig.23. Rotor active power (Pr1) and active power stored in or supplied by the ESS (Pess1) of WTG1.

VI. CONCLUSION

This paper has proposed a novel two-layer CPC scheme for a wind farm equipped with DFIG wind turbines. Simulation studies have been carried out for a wind farm equipped with 15 DFIG wind turbines to verify the effectiveness of the proposed CPC scheme. Results have shown that the proposed CPC scheme enabled the wind farm to effectively participate in unit commitment and active power and frequency regulations of the grid. The proposed system and control scheme provides a solution to help achieve high levels of penetration of wind power into electric power grids.

REFERENCES

[1] B. M. Han and G. G. Karady, "A new power conditioning system for superconducting magnetic energy storage," IEEE Trans. Energy Converse., vol. 8, no. 2, pp. 214–220, 1993.

[2]Liyan Qu, Wei Qiao, "Constant Power Control of DFIG Wind Turbines With Super capacitor Energy Storage" *IEEE Transactions On Industry Applications*, Vol. 47, No. 1, January/February 2011 359.

[3] "Focus on 2030: EWEA aims for 22% of Europe's electricity by 2030," *Wind Directions*, pp. 25–34, Nov./Dec. 2006.

[4] 20% Wind Energy By 2030: Increasing Wind Energy's Contribution to U.S. Electricity Supply, U.S. Department of Energy, Jul. 2008.

[5] Wind Generation & Total Load in the BPA Balancing Auth ority: DOE Bonneville Power Administration, U.S. Departmentof Energy.[Online].Available:http://www.transmission.bpa.gov/business/operations/Wind/default.aspx

[6] R. Piwko, D. Osborn, R. Gramlich, G. Jordan, D. Hawkins, and K. Porter, "Wind energy delivery issues: Transmission planning and competitive electricity market operation," *IEEE Power Energy Mag.*, vol. 3, no. 6, pp. 47–56, Nov./Dec. 2005.

[7] L. Landberg, G. Giebel, H. A. Nielsen, T. Nielsen, and H. Madsen, "Shortterm prediction—An overview," *Wind Energy*, vol. 6, no. 3, pp. 273–280, Jul./Sep. 2003.

[8] M. Milligan, B. Kirby, R. Gramlich, and M. Goggin, Impact of Electric Industry Structure on High Wind Peneration Potential, Nat. Renewable Energy Lab., Golden, CO, Tech. Rep. NREL/TP-55046273.[Online].Available:http://www.nrel.gov/docs/fy09osti/46273.pdf

[9] J. P. Barton and D. G. Infield, "Energy storage and its use with intermittent renewable energy," *IEEE Trans. Energy Convers.*, vol. 19, no. 2, pp. 441–448, Jun. 2004.

[10] D. Rastler, "Electric energy storage, an essential asset to the electric enterprise:Barriers and RD&D needs," *California Energy Commission Staff Workshop Energy Storage Technol., Policies Needed Support California's RPS Goals 2020*, Sacramento, CA, Apr. 2, 2009.

[11] M. G. Molina, P. E. Mercado, and E. H.Watanabe, "Dynamic performance of a static synchronous compensator with superconducting magnetic energy storage," in Proc. IEEE Power Electron. Spec. Conf., Jun. 2005, pp. 224–230.

[12] B. S. Borowy and Z. M. Salameh, "Dynamic response of a stand-alone wind energy conversion system with battery energy storage to wind gust,"*IEEE Trans. Energy Convers.*, vol. 12, no. 1, pp. 73–78, Mar. 1997.

[13] M.-S. Lu, C.-L. Chang, W.-J. Lee, and L. Wang, "Combining the wind power generation system with energy storage equipments," *IEEE Trans.Ind. Appl.*, vol. 45, no. 6, pp. 2109–2115, Nov./Dec. 2009.

AUTHOR DETAILS

V.KrishnaMurthy received the B.Tech degree from st.johns college of engineering and technology ,yemmiganur Affiliated to jntu ananthapur present he is perceive M.Tech(Electrical power engineering) from Narayana Engineering College ,Nellore. Affiliated to jntu Anantapur.

Ch.Rajesh Kumar received the Master degree in power electronics and drives from Sree sastha institute of engineering and technology Affiliated to Anna university Chennai, B.Tech degree from sri vidyanikethan engineering college Affiliated to Jntu Anantapur .Ragampet Tirupathi. Currently, He is Associate professor of electrical and electronics engineering at Narayana Engineering College, Nellore, AP.